Thermal Fluctuations of nano cantilevers for the detection of the biological particles modifications

E. Pierro [1], G. Carbone [2]
[1] University of Basilicata, School of Engineering,
Via dell'Ateneo Lucano 10, 85100, Potenza, Italy
e-mail: **elena.pierro@unibas.it**

[2] Polytechnic University of Bari, Department of Mechanics, Mathematics and Management,
V.le Japigia, 182, 70126, Bari, Italy

Abstract
Measuring the mechanical properties of biological particles, such as bacteria, viruses and cells, is becoming the most widespread method to monitor their metabolic changes which are at the basis of mutations or diseases. By properly coupling the bioparticles with nano resonators, constituted by simple mechanical systems like beams or disks at the nano scales, it is possible to retrieve their mode of vibrations, which represent the access key to crucial properties as the mass, the stiffness and the damping of these particles. Moving from the most recent studies in this field, which are mainly focused on the mass change detection by means of nano cantilever sensors, or present the stiffness and the modal damping measurement by exploiting optomechanical disk resonators, we present a theoretical study of the thermal vibrations of a nano cantilever, which is coupled with a particle, with the aim to disclosure more insights about the dynamical properties of this kind of biological system.

1 Introduction

In the medical-diagnostic field, the monitoring over time of certain tissue components, particles and cells is of fundamental importance [1-3]. There are a vast multitude of chemical and physical sensors capable of quantifying the concentration of pathogenic elements, and among the various most recent techniques in this field, the possibility of paying attention to the variation of bio-particles over time is particularly challenging. One of the possibilities for this purpose is the coupling of a particle, generally named as analyte, with a mechanical device, such as a disk or a cantilever, called analyzer or sensor, which has geometric dimensions comparable to those of the object under study. This is possible by virtue of the development of manufacturing techniques that allow the realization of micro devices with geometric characteristics of a few micrometers. It is precisely thanks to this, that the analyzer and analyte have comparable dimensions, that their resonance frequencies belong to the same frequency range, and the spectral content of the analyte is visible within the sensor response. However, a real coupling with micro cantilevers has not yet been proposed in the literature, and indeed it is possible to find works that use these mechanical devices only to measure the mass of the particles deposited above, through a frequency shift of the resonance peaks of the beams [4,5]. The principal reason besides this choice, lies in the cantilever dimensions, in particular the length of the beam up to now employed in this kind of applications, i.e. of about 100μm. However, it is quite immediate to observe that it is possible to make the resonances of the beam fall close to those of the particles of some typically analyzed bacteria, by means of cantilevers with lengths of a few micrometers. Infact, the first eigenfrequency of a spherical biological particle, is estimated to be [6]

$$\omega_p \sim \frac{1}{R_p}\sqrt{\frac{E_p}{\rho_p}} \tag{1}$$

being E_p the Young's modulus, ρ_p the density and R_p the radius of the particle. The natural frequencies of the flexural vibrations of a beam of length L are given by [7]

$$\omega_b = \frac{c_n^2}{L^2}\sqrt{\frac{EI}{A\rho}} = \frac{c_n^2}{2\sqrt{3}L^2}H\sqrt{\frac{E}{\rho}} \tag{2}$$

being $A = WH$ the rectangular cross section area, $I = WH^3/12$ the moment of inertia, c_n coefficients which specifically depend on the boundary conditions, i.e. for a cantilever beam $c_1 = 1.875$, $c_2 = 4.694$, $c_3 = 7.855$ for the first three modes. In order to be able to apply the Euler Bernoulli theory, we need to maintain $H/L \leq 0.1$, therefore we keep constant this ratio to 0.1. In Table 1 the values of the material properties and the geometrical characteristics are reported, for the biological particle considered in Ref. [6], and for a typical nano beam, which is suitable for the application here considered [8].

Table 1: Material properties and geometrical characteristics

Property	Numerical Value
E_p	5 GPa
ρ_p	2000 kg m^{-3}
R_p	0.45 μm
E	180 GPa
ρ	2300 kg m^{-3}
L	6 μm

These cantilevers, with length of the order of few μm, have recently been integrated into high-speed AFM controller [9], and allow to reach the MHz range. In particular, let us notice that the greater round shaped bioparticle, i.e. the bacterium, has a radius of about $0.450\mu m$ [6]. Bearing in mind that the goal of the study is to create a coupling between the resonances of the cantilever and the particle, which means having close their resonances, with the values shown in Table 1, we obtain the third flexural resonance of the beam $\omega_b = 502\ MHz$, while for the bio particle $\omega_p = 587\ MHz$. For all the reasonings made so far, it appears clear that the nano cantilever represents a valid alternative to the disk resonator, in its flexural vibrations. In this perspective, we present a theoretical study of the thermal vibrations of a nano cantilever coupled with a particle, by considering the analytical model presented by the authors [10], of a dAFM cantilever subjected to thermal fluctuations. We add a biological cell at the free end of the beam, and we model it by considering both the elastic properties and the viscosity induced by the surrounding fluid. The main advantage offered by the presented approach, is the possibility to investigate the modal coupling between the beam and the particle in a wide frequency range, not limiting the attention to a couple of resonances, as done in the studies found in the literature, where the sensor is modelled as a two degree of freedom system (see e.g. Ref. [6]). In this way, by observing the interaction of a greater number of resonances, more information about the dynamics of the bioparticle can be derived, in terms of its viscoelastic behaviour, and it is possible to pursue the goal by simply changing the length of the beam, thus adapting the sensor to different biological cells.

2 The cantilever-bioparticle system

2.1 The beam response

In this section we evaluate the thermal induced fluctuations of a cantilever immersed in a viscous fluid, which is coupled with a particle placed at its free end (Figure 1), and for this scope we employ the Fluctuation Dissipation Theorem (FDT), which states that the susceptibility function $\chi(x_1, x_2, t)$ of the cantilever, which is the displacement $w(x_1, \omega)$ at point x_1 due to the action of a concentrated unit force F at point x_2, is proportional to the time-derivative of the correlation function of the thermal fluctuations of the cantilever displacements [11]

$$\chi(x_1, x_2, t) = -\beta H(t)\frac{\partial}{\partial t}\langle w(x_1, 0)w(x_2, t)\rangle \tag{3}$$

being $\beta = (k_B T)^{-1}$ and k_B is Boltzmann's constant, T the absolute temperature and $H(t)$ is the Heaviside unit step function. In particular, we calculate the Cross Power Spectral Density (CPSD) $R(x_1, x_2, \omega) = \int dt\langle w(x_1, 0)w(x_2, t)\rangle exp(-i\omega t)$ of the cantilever thermal fluctuations, by means of the relation with the imaginary part of the time-Fourier transform of the susceptibility function, i.e. the imaginary part of the complex compliance $\chi(x_1, x_2, \omega) = \int dt\chi(x_1, x_2, t)exp(-i\omega t)$

$$R(x_1, x_2, \omega) = -\frac{2k_B T}{\omega} Im\chi(x_1, x_2, \omega) \tag{4}$$

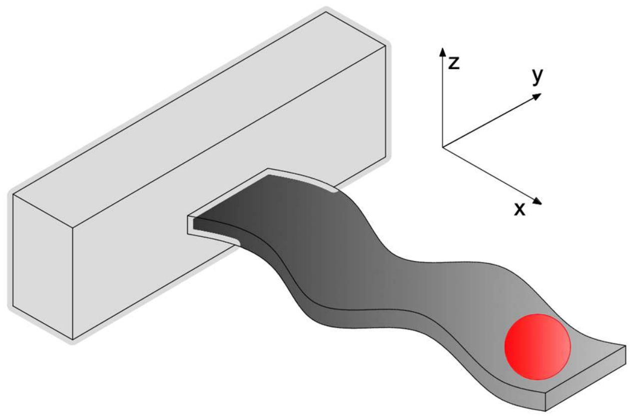

Figure 1: The nano-cantilever and the particle positioned at the free end.

Following the approach presented by the authors in Ref. [10], we solve the problem hereafter formulated

$$EI\frac{\partial^4\chi(x_1,x_2,t)}{\partial {x_1}^4} + [\rho A + \mu(x_1)]\frac{\partial^2\chi(x_1,x_2,t)}{\partial t^2} + c(x_1)\frac{\partial\chi(x_1,x_2,t)}{\partial t} +$$

$$+\alpha(x_1)\int_{-\infty}^{t}\frac{1}{\sqrt{t-\tau}}\frac{\partial^2\chi(x_1,x_2,\tau)}{\partial\tau^2}d\tau = \delta(x_1 - x_2)\delta(t) \tag{5}$$

where we define $c(x)$ the damping, $\alpha(x)$ the diffusive coefficient, and $\mu(x)$ the inertia term of the fluid response function $G(x, t) = -c(x) - \frac{\alpha(x)}{\sqrt{t}} - \mu(x)\delta(t)$, for $t > 0$, proposed in Ref. [10]. Let us observe that the $x -$ dependent distance of the cantilever cross sections from the wall is effective only when the beam is tilted, which is not the case considered in this study. Fourier transforming Eq. (5) we obtain

$$\frac{\partial^4\chi(x_1,x_2,\omega)}{\partial {x_1}^4} - B(x_1, \omega)^4\chi(x_1, x_2, \omega) = \delta(x_1 - x_2) \tag{6}$$

being $B(x, \omega)$ the following function

$$B(x, \omega) = \sqrt[4]{-\frac{i\omega c(x)-[\rho A+\mu]\omega^2+i\omega\ \alpha(x)\sqrt{i\omega\pi}}{EI}} \tag{7}$$

Equation (6) can be solved considering the equivalent problem given by the equation

$$\frac{\partial^4\chi(x_1,x_2,\omega)}{\partial {x_1}^4} - B(x_1, \omega)^4\chi(x_1, x_2, \omega) = 0 \tag{8}$$

with the boundary conditions

$$\chi^I(0, x_2, \omega) = \left.\frac{\partial\chi^I(x_1,x_2,\omega)}{\partial x_1}\right|_{x_1=0} = 0$$

$$[\chi(x_1, x_2, \omega)]_{x_1=x_2^-}^{x_1=x_2^+} = \left[\frac{\partial\chi(x_1, x_2, \omega)}{\partial x_1}\right]_{x_1=x_2^-}^{x_1=x_2^+} = \left[\frac{\partial^2\chi(x_1, x_2, \omega)}{\partial^2 x_1}\right]_{x_1=x_2^-}^{x_1=x_2^+} = 0$$

$$[\chi(x_1,x_2,\omega)]_{x_1=x_2^-}^{x_1=x_2^+} = \left[\frac{\partial\chi(x_1,x_2,\omega)}{\partial x_1}\right]_{x_1=x_2^-}^{x_1=x_2^+} = \left[\frac{\partial^2\chi(x_1,x_2,\omega)}{\partial^2 x_1}\right]_{x_1=x_2^-}^{x_1=x_2^+} = 0$$

$$\left[\frac{\partial^3\chi(x_1,x_2,\omega)}{\partial^3 x_1}\right]_{x_1=x_2^-}^{x_1=x_2^+} = 1$$

$$\left.\frac{\partial^2\chi^{II}(x_1,x_2,\omega)}{\partial^2 x_1}\right|_{x_1=L} = 0$$

$$\left.\frac{\partial^3\chi^{II}(x_1,x_2,\omega)}{\partial^3 x_1}\right|_{x_1=L} = -\frac{F_t}{EI} \tag{9}$$

The last condition of Eqs. (9) is related to the presence of the attached mass, i.e. the bio-particle, at the free end of the cantilever. By considering the particle attached to the beam section $x_1 = L$ by means of a spring of constant k_p and a viscous damper of constant c_p, as shown in Figure 2, the force exchanged between the particle and the beam can be written as a function of the thermal fluctuations of the cantilever displacements evaluated at the beam section $x_1 = x_2 = L$

$$F_t = F_{el} + F_d = k_p\bar{\xi}(\omega) + c_p s\bar{\xi}(\omega) = -EI\psi(\omega)\chi(L,L,\omega) \tag{10}$$

being $\bar{\xi}(\omega)$ the Fourier transform of the relative motion $\xi(t) = z(t) - w(L,t)$, and

$$\psi(\omega) = \frac{-(k_p+i\omega c_p)M_p\omega^2}{EI(-M_p\omega^2+i\omega c_p+k_p)} \tag{11}$$

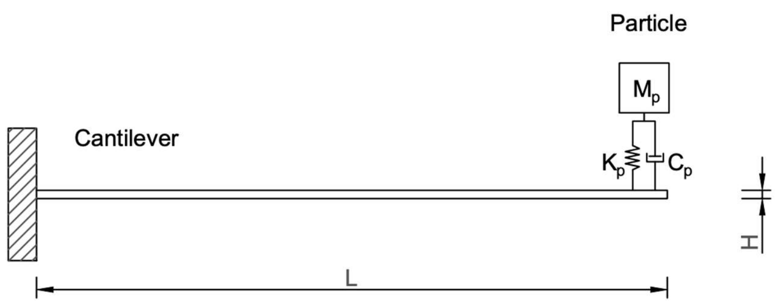

Figure 2: The schematic of the mechanical coupling between the nano-cantilever and the particle.

By following the procedure presented in Ref. [10], it is possible to calculate the Susceptibility Function in presence of a particle, which can be directly evaluated in correspondence of the free end section of the beam $x = L$

$$\chi(L,L,\omega) = \frac{cosh(BL)\,sin(BL) - cos(BL)\,sinh(BL)}{B^3 + cosh(BL)[B^3\,cos(BL) + \psi(\omega)\,sin(BL)] - \psi(\omega)\,cos(BL)\,sinh(BL)} \tag{12}$$

2.2 Dimensional Analysis

We define the frequency which will be considered as reference and that will be kept constant in the analysis

$$\bar{\omega} = \frac{1}{R_p}\sqrt{\frac{E}{\rho}} \tag{13}$$

The following non dimensional quantities are defined, $\tilde{E}_p = E_p/E$, $\tilde{\rho}_p = \rho_p/\rho$, $\widetilde{W} = W/R_p$, $\widetilde{H} = H/R_p$, $\tilde{L} = L/R_p$, $\Omega = \omega/\bar{\omega}$, $\tilde{\omega}_b = \omega_b/\bar{\omega}$. Regarding the natural frequency of the particle, we observe that

$$\omega_p = \bar{\omega}\sqrt{\frac{\tilde{E}_p}{\tilde{\rho}_p}} \tag{14}$$

thus the non-dimensional bio particle's resonance can be written as $\widetilde{\omega}_p = \omega_p/\bar{\omega} = \sqrt{\tilde{E}_p/\tilde{\rho}_p}$. This quantity will be considered as a parameter changing with $\tilde{E}_p$, maintaining the density $\tilde{\rho}_p$ constant, in order to taking into account the different resonances of the particle, once the radius R_p has been fixed too. Furthermore, it should be noticed that $k_p = \omega_p^2 M_p = M_p\bar{\omega}^2\tilde{E}_p/\tilde{\rho}_p$, and the viscous damping ratio $\zeta = c_p/(2M_p\omega_p) = \tilde{c}/(2\widetilde{\omega}_p)$, being $\tilde{c} = c_p/(M_p\bar{\omega})$. In this way, it is possible to write

$$\tilde{\psi}(\Omega, \widetilde{\omega}_p) = \psi R_p^3 = -\frac{16\pi\tilde{E}_p}{\tilde{W}\ \tilde{H}^3}\frac{1+i2\zeta\Omega/\widetilde{\omega}_p}{\left(-1+i2\zeta\frac{\widetilde{\omega}_p}{\Omega}+\frac{\widetilde{\omega}_p^2}{\Omega^2}\right)} \tag{15}$$

and

$$\tilde{\chi}(\tilde{L},\tilde{L},\Omega) = \frac{cosh(\tilde{B}\tilde{L})\,sin(\tilde{B}\tilde{L})-cos(\tilde{B}\tilde{L})\,sinh(\tilde{B}\tilde{L})}{\tilde{B}^3+cosh(\tilde{B}\tilde{L})[\tilde{B}^3\,cos(\tilde{B}\tilde{L})+\tilde{\psi}\,sin(\tilde{B}\tilde{L})]-\tilde{\psi}\,cos(\tilde{B}\tilde{L})\,sinh(\tilde{B}\tilde{L})} \tag{16}$$

being $\tilde{B} = BR_p$ and $\tilde{\chi} = \chi/R_p^3$.

3 Results

In this section, we show the results obtained with the model here presented, by considering the width W of the beam constant, which needs to satisfy the Euler Bernoulli hypothesis, i.e. $L >> W$. Following the aforementioned considerations, and taking the material and geometrical properties of Table 1, we set $W = 0.6\ \mu m$. This quantity is fundamental to calculate the coefficients of the drag force exerted by the fluid on the cantilever, as shown in Ref. [10], and in this case they are evaluated in air at the free end of the cantilever, far from the substrate, as $c = 78.78 * 10^{-6}\mathrm{kg(m\ s)^{-1}}$, $\alpha = 3.33 * 10^{-8}\mathrm{kg(m\ s^{-1/2})^{-1}}$, and $\mu = 5.72 * 10^{-12}\mathrm{kg\ m^{-1}}$. They have been determined by finding the best fitting with the existing accurate computational fluid dynamics non-dimensional solutions of a 2D fluid flowing around a vibrating rectangular cross-section [12].

In Figure 3, the PSD of the cantilever tip deflection is shown, $\tilde{S}(\Omega) = -Im\tilde{\chi}(\tilde{L},\tilde{L},\Omega)/\Omega$, for three different values of the parameter $\tilde{E}_p$, and for $\zeta = \bar{\zeta} = 0.018$. We point out that changing the value of $\tilde{E}_p$ is equivalent to considering in this study different resonance frequencies of the particle, therefore associated with different modes of vibration of the particle. Figure 3 highlights that, depending on the elastic moduli of both the particle and the cantilever, three different regimes can be observed, i.e. an insensitive regime for $\tilde{E}_p \ll \bar{E}_p$ (Figure 3-a), a coupling regime for $\tilde{E}_p \cong \bar{E}_p$ (Figure 3-b) and an inertial regime for $\tilde{E}_p \gg \bar{E}_p$ (Figure 3-c), being $\bar{E}_p = E_p/E$ obtained with the numerical values in Table 1.

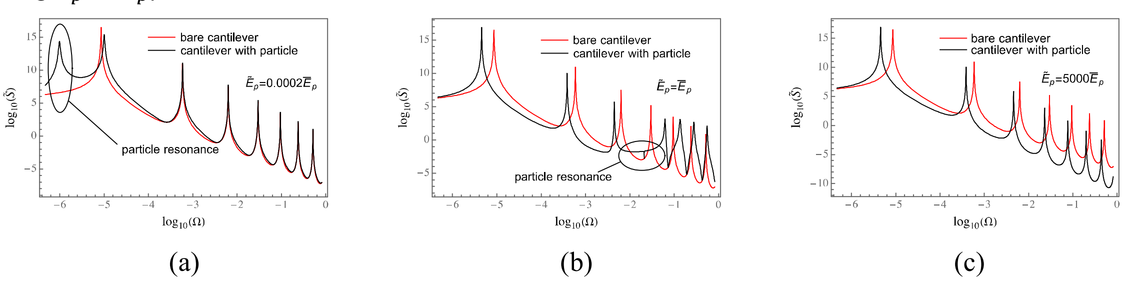

Figure 3: The thermal power spectrum of the bare cantilever (red lines) and of the cantilever with the particle at the free end (black lines), for three different values of the ratio $\tilde{E}_p$.

It should be noticed that the coupling regime is rather wide, since we are considering the complete vibrational response of the cantilever, and therefore a greater number of resonance peaks could potentially be nearby the first resonance of the particle. This circumstance is very useful for the application, since we gain greater flexibility in the characterization of nanoparticles, in comparison with models recently presented (e.g. Ref.[6]) which schematize the analyzer with a few degrees of freedom.

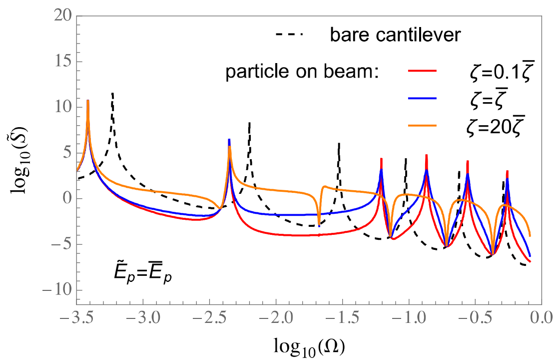

Figure 4: The thermal power spectrum of the bare cantilever (black dashed lines) and of the cantilever with the particle at the free end, for three different values of ζ.

Furthermore, the model presented here allows us to capture the amount of the viscous damping of the particle under analysis, in correspondence with one of its modes of vibration. This is clearly shown in Figure 4, where the PSD of the cantilever tip deflection exhibits profound variations in its shape, as the damping factor ζ associated with the particle varies. Worthy of note is the fact that, regardless of the internal damping of the particle, its presence creates a sort of "watershed" effect, moving away from itself the resonance peaks of the beam, present both on the right and on the left. However, beyond this fundamental effect, it could be very useful to be able to "see" the peak associated with the particle, in addition to those of the beam. Actually it is not always pronounced (see Figure 3-b, black curve), but one way to enhance it in the PSD curve, once the physical characteristics of the particle in terms of damping and stiffness have been fixed, is to slightly vary the length of the beam. In Figure 5 we can notice that by increasing the beam length, for the particular numerical values considered (Table 1) which give $\bar{L} = L/R_p$, the resonance associated to the particle is more prominent (see in particular the orange curve in Figure 5, obtained for $\tilde{L} = 1.2\bar{L}$).

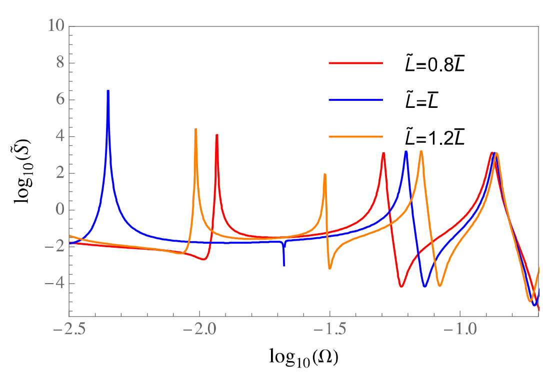

Figure 5: The thermal power spectrum of the cantilever with particle, for different values of the beam length.

In conclusion, the analytical model presented in this work shows to possess all the necessary requirements for the control and the tuning of the coupling between the beam-analyzer and the particle-analyte, simply by selecting appropriate values of the cantilever length. Moreover, through a continuous model, it is easier to capture the dynamics of particles with different mechanical properties, in terms of stiffness and damping, which may change during the life of the particle, as it happens in the biological cells, especially in the case of their damage during an ongoing disease. A further element of flexibility of the analytical model, which will be investigated in future studies, concerns the possibility of considering the beam system with particle immersed in a fluid. At a computational level, it will be sufficient to calculate the new coefficients of the drag force exerted by the considered fluid, as previously shown by the authors in Ref. [10]. Some further reasoning will be necessary regarding the quantity of fluid that the particle can absorb, modifying its properties also from a dynamic point of view.

4 Conclusions

This paper presents an analytical model able to describe the dynamical interaction between a nano cantilever and a biological particle, which is considered deposited on the free and of the beam. Through a recent model of the fluid drag presented by the authors, it has been possible to evaluate the PSD of this system, which clearly shows the presence of the particle in the frequency domain. Compared to all the cantilever sensor models presented in the literature so far, which consider beam lengths several orders of magnitude larger than the particles with which they interact, the model here presented considers geometric values of the beam comparable to those of the particle, taking inspiration from recent mechanical disk resonators which exploit the latest manufacturing technologies to create such miniaturized devices. We have shown how a simple cantilever is able to capture the dynamics of the particle very precisely, through our accurate and recently experimentally validated analytical model. The approach, compared to the lumped parameter models of mechanical resonators presented so far, allows us to track the variation of the mechanical characteristics of the particle. This condition opens up an interesting scenario for the creation of a new generation of markers for biological cells that tend to change over time, under the action of damage caused by possible diseases.

References

[1] C. Cafolla, J. P. Robson, A. Elbourne, K. Voïtchovsky, "Quantitative Detection of Biological Nanovesicles in Drops of Saliva Using Microcantilevers", *ACS Appl. Mater. Interfaces*, vol. 16, pp. 44−53, 2024.

[2] P. M. Kosaka, M. Calleja, J. Tamayo, "Optomechanical devices for deep plasma cancer proteomics", *Seminars in Cancer Biology*, vol. 52, pp. 26–38, 2018.

[3] B. Péter, E. Farkas, S. Kurunczi, Z. Szittner, S. Bősze, J.J. Ramsden, I. Szekacs and R. Horvath, "Review of Label-Free Monitoring of Bacteria: From Challenging Practical Applications to Basic Research Perspectives", *Biosensors*, vol. 12, no. 4, 2022.

[4] O. Malvar, J.J. Ruz, P.M. Kosaka, C.M. Domınguez, E. Gil-Santos, M. Calleja and J. Tamayo, "Mass and stiffness spectrometry of nanoparticles and whole intact bacteria by multimode nanomechanical resonators", *Nat Commun* vol.7, 13452, 2016.

[5] S. Dohn, W. Svendsen, A. Boisen, and O. Hansen, "Mass and position determination of attached particles on cantilever based mass sensors", *Rev Sci Instrum*, vol. 78, 103303, 2007.

[6] E. Gil-Santos, J.J. Ruz, O. Malvar, et al., "Optomechanical detection of vibration modes of a single bacterium", *Nat. Nanotechnol.,* vol. 15, pp. 469–474, 2020.

[7] Thomson, W.T. and Dahleh M.D., *Theory of Vibration with Applications*. 5th edition. Englewood Cliffs, NJ: Prentice Hall, 1997.

[8] Z. J. Davis and A. Boisen, "Aluminum nano-cantilevers for high sensi- tivity mass sensors", in 5th *IEEE Conference on Nanotechnology*, 2005, IEEE.

[9] J.D. Adams, A. Nievergelt, B.W. Erickson, C. Yang, M. Dukic, G.E. Fantner, "High-speed imaging upgrade for a standard sample scanning atomic force microscope using small cantilevers", *Rev Sci Instrum,* vol 85, no.9, 2014.

[10] E. Pierro, F. Bottiglione, G. Carbone, "Thermal Fluctuations and Dynamic Modeling of a dAFM Cantilever", *Advanced Theory and Simulations*, vol.2, no. 5, 2019.

[11] D.Chandler, *Introductionto Modern Statistical Mechanics*. Oxford University Press, NewYork, 1987.

[12] R. J. Clarke, S. M. Cox, P. M. Williams, O. E. Jensen, “The drag on a microcantilever oscillating near a wall”, *J. Fluid Mech.*, vol. 545, 397, 2005.